HHS Public Access

Author manuscript

Eur J Med Chem. Author manuscript; available in PMC 2018 July 07.

Published in final edited form as:

Eur J Med Chem. 2017 July 07; 134: 62–71. doi:10.1016/j.ejmech.2017.04.001.

Identification of novel 2-(benzo[*d*]isoxazol-3-yl)-2-oxo-*N*-phenylacetohydrazonoyl cyanide analogues as potent EPAC antagonists

Na Ye[a,c,1], **Yingmin Zhu**[b,1], **Zhiqing Liu**[a], **Fang C. Mei**[b], **Haiying Chen**[a], **Pingyuan Wang**[a], **Xiaodong Cheng**[b,**], and **Jia Zhou**[a,*]

[a]Chemical Biology Program, Department of Pharmacology and Toxicology, University of Texas Medical Branch, Galveston, Texas 77555, United States

[b]Department of Integrative Biology and Pharmacology, Texas Therapeutics Institute, The University of Texas Health Science Center, Houston, Texas 77030, United States

[c]Department of Medicinal Chemistry, College of Pharmaceutical Sciences, Soochow University, Suzhou, Jiangsu 215123, China

Abstract

Two series of novel EPAC antagonists are designed, synthesized and evaluated in an effort to develop diversified analogues based on the scaffold of the previously identified high-throughput (HTS) hit **1** (**ESI-09**). Further SAR studies reveal that the isoxazole ring A of **1** can tolerate chemical modifications with either introduction of flexible electron-donating substitutions or structurally restrictedly fusing with a phenyl ring, leading to identification of several more potent and diversified EPAC antagonists (e.g., **10 (NY0617), 14** (**NY0460**), **26** (**NY0725**), **32** (**NY0561**), and **33** (**NY0562**)) with low micromolar inhibitory activities. Molecular docking studies on compounds **10** and **33** indicate that these two series of compounds bind at a similar site with substantially different interactions with the EPAC proteins. The findings may serve as good starting points for the development of more potent EPAC antagonists as valuable pharmacological probes or potential drug candidates.

Graphical abstract

*Corresponding author: Jia Zhou, PhD, Chemical Biology Program, Department of Pharmacology and Toxicology, University of Texas Medical Branch, Galveston, Texas 77555, United States, Tel: (409) 772-9748; Fax: (409) 772-9648; jizhou@utmb.edu.

**Corresponding author: Xiaodong Cheng, PhD, Department of Integrative Biology and Pharmacology, Texas Therapeutics Institute, The University of Texas Health Science Center Houston, Texas 77030, United States, Tel: (713) 500-7487; Fax: (409) 500-7465, xiaodong.cheng@uth.tmc.edu.

[1]These authors contribute equally to this work.

Notes

The authors declare no competing financial interest.

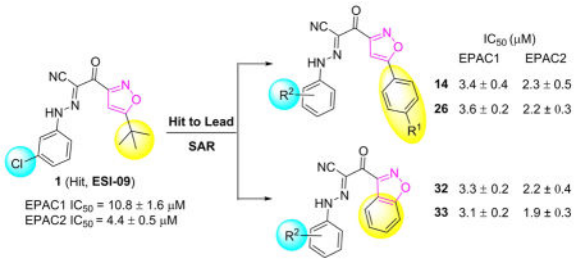

Keywords

Exchange proteins directly activated by cAMP; EPAC; antagonist; molecular docking

1. Introduction

Exchange proteins directly activated by cAMP (EPACs) were first identified as novel intracellular effector proteins of cyclic adenosine monophosphate (cAMP) by two independent groups in 1998 [1, 2]. Prior to the discovery of EPAC proteins, the major physiological effects of cAMP in mammalian cells are believed to be transduced by the classic protein kinase A/cAMP-dependent protein kinase (PKA/cAPK), and cyclic nucleotide-activated ion channels (CNG and HCN) in certain tissues [3–6]. Between two ubiquitously expressed intracellular cAMP receptor families, EPAC proteins, unlike PKA, have no kinase activity but act as guanine nucleotide exchange factors to catalyze the exchange of GDP with GTP for the down-stream small GTPases, Rap1 and Rap2, in response to intracellular cAMP [1, 2]. Two structurally homologous but functionally nonredundant isoforms of mammalian EPAC proteins have been identified, EPAC1 and EPAC2. EPAC1 is more ubiquitously expressed, whereas the expression of EPAC2 is relatively restricted, mainly found in brain, pancreatic islets and adrenal gland [2]. From nearly two decades of research on EPAC, accumulating studies, including those with the aid of small-molecule EPAC modulators [7, 8] such as various cAMP analogues (e.g. 007-AM [9]) and newly discovered EPAC-specific antagonists (e.g. ESI-09 [10–14]), have demonstrated that EPAC proteins play important roles in insulin secretion, energy homeostasis, cardiovascular response, pain sensing, osteoclast differentiation, neurotransmitter release, Treg-mediated immune suppression, integrin-mediated cell adhesion, cell migration and proliferation, cell exocytosis, and apoptosis as well as gene transcription and chromosomal integrity [15–19], and thus represent potential therapeutic targets for various human diseases such as cancer, bacterial and viral infections, chronic pain, diabetes, obesity, and heart failure.

Our previous high-throughput screening (HTS) campaign using automated, robust, and sensitive fluorescence based competition assay [10, 11] led to the identification of several EPAC specific inhibitors (ESIs), and was subsequently followed by extensive hit-to-lead optimizations [20–24]. Among these identified inhibitor hits, **ESI-09** (**1**, Fig. 1) has been shown to selectively inhibit EPAC functions *in vitro* [12] and *in vivo* [13, 14]. With the aid of molecular docking studies of **1** into the cAMP binding domain B of active EPAC2 proteins, we hypothesized that binding interactions of inhibitors to EPAC2 proteins may

primarily occur through two terminal hydrophobic pockets (P1 and P2) and the unique linker [7]. Later, systematic structure-activity–relationships (SARs) studies were performed, leading to the discovery of several more active EPAC antagonists (e.g., **2** (NY0123)) with low micromolar inhibitory activity and improved solubility [24].

In a continuing effort to develop novel diversified analogues based on the scaffold of hit **1**, we focus on our further chemical optimizations involving modifications of 5-*tert*-butyl group on the isoxazole ring A, meanwhile retaining favorable hydrophobic fragments of EPAC antagonists including fluorine-substitutions on the B-ring identified from our previous studies [24]. In order to explore the depth of the aforementioned hydrophobic pocket P2, as depicted in Fig. 1, series I was designed by inserting a rigid phenyl ring between the isoxazole A ring and its *tert*-butyl substitution at the 5-position. For comparison, we also attempted to make the molecular skeleton more compacted by fusing a phenyl ring with the isoxazole A (as depicted in series II, Fig. 1). Herein, we report such structural modifications of compound **1** with a focus on improving EPAC inhibitory activities and structural diversity of EPAC antagonists. The studies have resulted in the discovery of several novel potent EPAC antagonists such as **14** (**NY0460**), **26** (**NY0725**), **32** (**NY0561**), and **33** (**NY0562**), with low micromolar inhibitory activities for preclinical development.

2. Results and discussion

2.1. Chemistry

The synthesis of new derivatives based on 2-(isoxazol-3-yl)-2-oxo-*N*′-phenyl-acetohydrazon-oyl cyanide scaffold with chemical optimizations of 5-*tert*-butyl group on the isoxazole is outlined in Scheme 1. Various ethyl isoxazole-3-carboxylates **3a–f** were used as the key intermediates. **3a–f** were prepared either from the commercially available pinacolones and oxalic acid diethyl esters in two steps as previously described by us [20, 24], or from ethyl esterification of the commercially available isoxazole-3-carboxylic acids. Ethyl esters **3a–f** were first converted into the corresponding ketonitriles **4a–f** by the treatment of MeLi and CH_3CN using our previously reported protocols [20, 23]. By further modifications of Kowalsko's reaction, NaH was used instead of MeLi as the base under a milder condition to generate the corresponding ketonitriles from ethyl esters **3a–f** in good yields. On the other hand, aromatic amines **5a–h** were treated with sodium nitrite and 2 N hydrochloric acid to give the corresponding aryldiazonium chlorides **6a–h**. The aryldiazonium salts **6a–h** with the crude cyanomethyl ketones **4a–f** were then directly coupled in the presence of NaOAc as the catalyst at 0 °C afforded new derivatives of series I compounds **7**–**27** in 14–81% yields for two steps from **4a–f** (Scheme 1). The desired products of series II **30–37** were accomplished from the commercially available ethyl benzo[d]isoxazole-3-carboxylate **28** with two steps in a similar fashion to those described for the synthesis of Series I.

2.2. Biology

2.2.1 In Vitro Evaluation of EPAC1 Inhibition—To explore the SARs and examine how the modifications on the isoxazole ring affect biological activities of newly synthesized analogues, we first evaluated their ability to inhibit EPAC1-mediated Rap1b-bGDP exchange

activity using purified recombinant full-length EPAC1 proteins. Previous hit **1** was used as the reference compound, with an IC_{50} value of 10.8 μM in inhibiting EPAC1 [25].

As shown in Table 1, we initially investigated the effect of the inserted phenyl ring between 5-*tert*-butyl group and isoxazole ring A of hit **1** in series I, leading to compound **7** with an IC_{50} value of 8.6 μM, which has a slight increase of inhibitory activity in comparison with that of **1**. Given that fluorine substitutions may have an important contribution to the improvement of metabolic stability, solubility and bioactivity, as found in our previous publications [24, 26], selected fluorine substitutions on B ring were introduced to newly designed compounds **8–11**. 3,5-di-CF_3-substituted analogue **11** results in a slight loss of activity, while compound **10** with 3-CF_3,4-Cl-substitution displays an enhanced potency, with an IC_{50} value of 7.3 μM. To evaluate the importance of 4-*tert*-butyl group on the inserted phenyl ring, we attempted the removal of this moiety, leading to new analogues **13–15**. To our delight, compounds **13–15**, not only have a better solubility than our previously reported compound **12** [24], but also exhibit an improved potency compared to that of 4-^{t}Bu-phenyl substituted analogues. This indicates that 4-^{t}Bu group on the inserted phenyl ring is dispensable for its activity. The most potent one of this series, 3-CF_3,4-Cl-substituted compound **14** (Fig. 2), is about 5-fold increase in potency when compared to that of **1**, with an IC_{50} value of 2.4 μM and as potent as previously reported lead compound **2**. We next explored the electronic effect of substitutions at the 4-position of the inserted phenyl ring. Compounds **16–24** all result in a loss of activity. However, compounds **22–24** with other electron-donating groups such as methoxy, are more potent than corresponding compounds **16–21** with other electron-withdrawing groups such as fluoro and chloro. Particularly, 4-methoxy substituted analogues **23** and **24** display good activities, with the same IC_{50} values of 5.6 μM. As expected, replacement of 4-methoxy phenyl on the isoxazole ring A with its bioisostere, more electron-donating furan-2-yl group (as in compounds **25–27**), also leads to an increase of activity. The most potent one of them, **25**, shows an IC_{50} value of 3.6 μM. These results suggest that the 5-position of the isoxazole ring A is more suitable for chemical modifications and favorable with electron-donating groups.

In series II as shown in table 2, replacement of isoxazole ring A of **1** with benzo[*d*]isoxazol moiety (as in compound **30**), results in a slight loss of potency when compared to that of **1**, with an IC_{50} value of 13.2 μM. However, further installation of fluorine-containing groups on its B ring quickly boosts the activity, except 3-Cl,5-F and 3,4,5-tri-F groups (as in compounds **34** and **37**). Compounds **31–33** result in approximately 2~4-fold increase in potency when compared to that of **1**, with IC_{50} values of about 2–4 μM (Fig. 2). Compound **33** has a substantially different new scaffold from that of previously described lead compound **2**, but displays a comparable potency with an IC_{50} value of 2.7 μM.

All these findings suggest that the isoxazole ring A of **1** can tolerate chemical modifications with either introduction of electron-donating substitutions or restrictedly fusing with a phenyl ring.

2.2.2 In Vitro Evaluation of EPAC2 Inhibition—From the biological results discussed above, compounds **10**, **14–15**, **23–24**, **26–27**, and **31**–**32** were identified as potent EPAC1 inhibitors with IC_{50} values lower than 8 μM and more potent than reference compound **1**.

Consistently, these selected compounds together with hit **1** were further evaluated for their ability to inhibit EPAC2-mediated Rap1b-bGDP exchange activity, rather than using previously described sensitive fluorescence based competition assay which may be interfered with their autoflorescence of these two series of compounds [24–25]. As shown in Table 3, the previous hit **1** is 2.5-fold more potent on EPAC2 inhibition than that on EPAC1, with an IC_{50} value of 4.4 μM. Interestingly, most of our selected, newly synthesized analogues exhibit significantly enhanced potency compared to that of **1**, except compounds **23** and **24** (Fig. 3). Among these, compound **33** exhibits the best inhibitory activity for EPAC2, with an IC_{50} value of 1.9 μM (Fig. 3). Compounds such as **14**, **26** and **32–33** with IC_{50} values lower than 4 μM for both EPAC1 and EPAC2 may serve as valuable pharmacological tools to probe the functions of EPAC in diseases or as potential drug candidates for further preclinical development.

2.3. Predicted Binding Modes of Compounds 10 and 33 with the cAMP Binding Domain B (CBD-B) of EPAC2 Proteins

Due to the lack of the X-ray cocrystal structures of our newly synthesized small molecules and their targeted proteins, molecular docking studies as useful methods may help us better understand the structure–activity relationships of these new compounds toward EPACs. Given the only available X-ray crystal structures of inactive and active EPAC2 proteins [27, 28], molecular docking studies of compounds **1**, **10** and **33** at CBD-B of active EPAC2 protein (PDB Code 3CF6) were performed to investigate the predicted binding modes using the Schrödinger Small-Molecule Drug Discovery Suite [23]. Although this algorithm slightly differs from our previously employed AutoDock Vina [7, 24], the docking results are generally consistent with the previous studies. The current docking results also reveal that these new compounds fit well into the functional CBD-B binding pocket of active EPAC2 (Fig. 4A). As shown in Fig. 4B, the molecular docking studies of **10** comply with our previous results with hit **1** through the overlay analysis of two ligands. The isoxazolyl moiety and the 3-CF_3-4-Cl-phenyl fragment of **10** respectively extend to two previously supposed hydrophobic pockets, while this binding mode is further stabilized by the occurrence of one hydrogen bond between the oxygen atom in carbonyl group of the linker and residue L406, as well as one halogen bond between the chloro atom in the 3-CF_3-4-Cl-phenyl fragment and residue E451 (Figure 4C). Interestingly, compound **33** interacts with EPAC2 protein in a substantially different manner from that of compounds **1** and **10** (Figs. 4A and 4D). Its interactions with EPAC2 are dominated by the three strong hydrogen bonds and one halogen bond, including the oxygen atom in the benzo[*d*]isoxazol moiety with residue L406, the chloro group in phenyl fragment with residue N445, and the nitrogen atom in cyano group of the linker with K450 as well as its hydrogen atom with R448, in addition to the aforementioned hydrophobic interactions. These molecular docking studies could also reasonably explain why these two series of compounds with unique linkers might have better EPAC2 inhibitory activity (Figs. 4C and 4D). It is worth mentioning that this new scaffold as in compound **33**, where the nitrogen atom on the heteroaryl ring forms a hydrogen bond with residue L406, may offer a good starting point for further drug design and structural optimizations.

3. Conclusions

Two series of novel EPAC antagonists based on the scaffold of the previously identified high-throughput hit **1** (**ESI-09**) have been designed, synthesized, and biologically evaluated for their EPAC1 and EPAC2 inhibitory activities. The SAR results based on EPAC2 activity comply with our docking studies in general, indicating that the isoxazole ring B of **1** can tolerate chemical modifications with either introduction of flexible electron-donating substitutions or structurally restrictedly fusing with a phenyl ring. The new scaffold of series II, as in compound **33** interacting with EPAC2 in a novel binding mode, may offer a good starting point for further drug design and structural optimizations. All these modification efforts allow us to further tune the original hit **1** to achieve more potent and structurally diverse EPAC1 and EPAC2 inhibitors, such as **10 (NY0617), 14** (**NY0460**), **26** (**NY0725**), **32** (**NY0561**), and **33** (**NY0562**) with IC_{50} values in the low micromolar range. These compounds may hold promise as potential drug candidates toward novel therapeutics against human diseases, and serve as valuable pharmacological probes to elucidate the physiological functions of EPAC proteins. Currently, the *in vitro* and *in vivo* activities of these selected compounds in infectious disease models (e.g. rickettsiosis) are being investigated. Further systematic optimizations based upon identified new scaffolds of these two series toward EPAC subtype selectivity are also under way and the findings will be reported in due course.

4. Experimental section

4.1. Chemistry

All commercially available starting materials and solvents were reagent grade, and used without further purification. Reactions were performed under a nitrogen atmosphere in dry glassware with magnetic stirring. Preparative column chromatography was performed using silica gel 60, particle size 0.063–0.200 mm (70–230 mesh, flash). Analytical TLC was carried out employing silica gel 60 F254 plates (Merck, Darmstadt). Visualization of the developed chromatograms was performed with detection by UV (254 nm). NMR spectra were recorded on a Bruker-600 or Bruker-300 (^{1}H, 600 & 300 MHz; ^{13}C, 150 & 75 MHz) spectrometer. ^{1}H and ^{13}C NMR spectra were recorded with TMS as an internal reference. Chemical shifts were expressed in ppm, and *J* values were given in Hz. High-resolution mass spectra (HRMS) were obtained from Thermo Fisher LTQ Orbitrap Elite mass spectrometer. Parameters include the following: Nano ESI spray voltage was 1.8 kV; Capillary temperature was 275 °C and the resolution was 60,000; Ionization was achieved by positive mode. Melting points were measured on a Thermo Scientific Electrothermal Digital Melting Point Apparatus and uncorrected. Purities of final compounds were established by analytical HPLC, which was carried out on a Shimadzu HPLC system (model: CBM-20A LC-20AD SPD-20A UV/VIS). HPLC analysis conditions: Waters μBondapak C18 (300 × 3.9 mm); flow rate 0.5 mL/min; UV detection at 270 and 254 nm; linear gradient from 10% acetonitrile in water to 100% acetonitrile in water in 20 min followed by 30 min of the last-named solvent (0.1% TFA was added into both acetonitrile and water). All biologically evaluated compounds are > 95% pure.

4.1.1. N-(3-Chlorophenyl)-2-(5-(4-(tert-butyl)phenyl)isoxazol-3-yl)-2-oxoacetohydrazonoyl cyanide (7)—To a solution of CH_3CN (0.43 mL, 7.32 mmol) in anhydrous THF (10 mL) was added 1.6 M methyl lithium in diethyl ether (2.30 mL, 3.66 mmol) at −78 °C under nitrogen. The mixture was stirred at −78 °C for 0.5 h, and ethyl 5-(4-(*tert*-butyl)phenyl)isoxazole-3-carboxylate **3a** (500 mg, 1.83 mmol) in THF (10 mL) was then added dropwise. The solution was stirred at −78 °C for 1 h and then quenched with acetic acid (0.21 mL, 3.66 mmol). The mixture was warmed to 0 °C and poured onto ice/water (10 mL) and extracted with ethyl acetate (20 mL). The organic lay was dried over Na_2SO_4, filtered and concentrated under reduced pressure. The crude residue **4a** (330 mg, 75%) was obtained as a white solid and directly used for next step without further purification. ^{1}H NMR (300 MHz, $CDCl_3$) δ 7.74 (d, *J* = 8.4 Hz, 2H), 7.53 (d, *J* = 8.4 Hz, 2H), 6.92 (s, 1H), 4.25 (s, 2H), 1.32 (s, 9H).

To a solution of 3-chloroaniline **5a** (37 mg, 0.33 mmol) in H_2O (10 mL cooled to −5 °C) was added 0.2 mL of 2 N HCl (aq.). To the resulting acidic aniline solution, 1 N solution of sodium nitrite (0.33 mL, 0.33 mmol) was added dropwise to generate the aryldiazonium salt solution **6a**. To the aryldiazonium salt solution was added sodium acetate (54 mg, 0.66 mmol), followed by 1 mL solution of crude 3-oxo-3-(3-phenylisoxazol-5-yl)propanenitrile **4a** (88 mg, 0.33 mmol) in ethanol. The reaction mixture was stirred at 0 °C for 5 min, and then poured onto H_2O (10 mL) and extracted with ethyl acetate (20 mL). The organic layer was dried over Na_2SO_4, filtered and concentrated under reduced pressure. The residue was purified by short column chromatography on silica gel, eluting with hexane/ethyl acetate (2/1) to provide the desired product **7** (67 mg, 50% for two steps from **3a**) as a yellow solid. ^{1}H NMR (300 MHz, DMSO-*d*$_6$) δ 7.90 (d, *J* = 8.4 Hz, 2H), 7.59 (d, *J* = 8.4 Hz, 3H), 7.54 – 7.45 (m, 2H), 7.43 (s, 1H), 7.25 (d, *J* = 7.2 Hz, 1H), 1.32 (s, 9H). ^{13}C NMR (75 MHz, DMSO-*d*$_6$) δ 179.41, 170.22, 161.42, 154.25, 144.10, 134.44, 131.73, 126.63, 126.17, 125.65, 124.03, 117.18, 116.11, 113.84, 101.39, 35.19, 31.32. HRMS (ESI) calcd for $C_{22}H_{20}ClN_4O_2$ 407.1275 $(M + H)^+$, found 407.1270.

4.1.2. N-(3-Chloro-5-(trifluoromethyl)phenyl)-2-(5-(4-(tert-butyl)phenyl)isoxazol-3-yl)-2-oxoacetohydrazonoyl cyanide (8)—Compound **8** was prepared in 22% yield (two steps from **3a**) by a procedure similar to that used to prepare compound **7**. The title compound was obtained as a yellow solid. ^{1}H NMR (300 MHz, DMSO-*d*$_6$) δ 7.88 (d, *J* = 8.4 Hz, 2H), 7.78 (s, 2H), 7.62 (s, 1H), 7.58 (d, *J* = 8.4 Hz, 2H), 7.42 (s, 1H), 1.32 (s, 9H). ^{13}C NMR (75 MHz, DMSO-*d*$_6$) δ 179.13, 170.04, 166.63, 154.17, 135.45, 132.13 (q, *J* = 33.7 Hz), 126.57, 126.09, 125.33, 124.10, 121.42, 121.16, 113.32, 101.48, 35.17, 31.32. HRMS (ESI) calcd for $C_{23}H_{19}F_3ClN_4O_2$ 475.1149 $(M + H)^+$, found 475.1145.

4.1.3. N-(3-Chloro-4-(trifluoromethyl)phenyl)-2-oxo-2-(5-(4-(tert-butyl)phenyl)isoxazol-3-yl)acetohydrazonoyl cyanide (9)—Compound **9** was prepared in 28% yield (two steps from **3a**) by a procedure similar to that used to prepare compound **7**. The title compound was obtained as a yellow solid. ^{1}H NMR (300 MHz, DMSO-*d*$_6$) δ 7.92 – 7.86 (m, 3H), 7.71 (s, 1H), 7.59 (m, 3H), 7.39 (s, 1H), 1.33 (s, 9H). ^{13}C NMR (75 MHz, DMSO-*d*$_6$) δ 179.17, 169.93, 161.89, 154.15, 132.22, 129.66, 126.61,

126.13, 124.14, 119.99, 116.73, 115.06, 101.43, 35.18, 31.33. HRMS (ESI) calcd for $C_{23}H_{19}F_3ClN_4O_2$ 475.1149 $(M + H)^+$, found 475.1140.

4.1.4. N-(4-Chloro-3-(trifluoromethyl)phenyl)-2-oxo-2-(5-(4-(tert-butyl)phenyl)isoxazol-3-yl)acetohydrazonoyl cyanide (10)—Compound **10** was prepared in 41% yield (two steps from **3a**) by a procedure similar to that used to prepare compound **7**. The title compound was obtained as a yellow solid. ^{1}H NMR (300 MHz, DMSO-d_6) δ 8.00 (d, J = 2.2 Hz, 1H), 7.88 (d, J = 8.5 Hz, 2H), 7.75 (m, 2H), 7.59 (d, J = 8.5 Hz, 2H), 7.41 (s, 1H), 1.33 (s, 9H). ^{13}C NMR (75 MHz, DMSO-d_6) δ 179.21, 170.08, 161.68, 154.17, 133.34, 127.93 (q, J = 31.0 Hz), 126.59, 126.09, 124.79, 124.07, 122.48, 116.81, 114.22, 101.33, 35.18, 31.33. HRMS (ESI) calcd for $C_{23}H_{19}F_3ClN_4O_2$ 475.1149 $(M + H)^+$, found 475.1147.

4.1.5. N-(3,5-Bis(trifluoromethyl)phenyl)-2-(5-(4-(tert-butyl)phenyl)isoxazol-3-yl)-2-oxoacetohydrazonoyl cyanide (11)—Compound **11** was prepared in 26% yield (two steps from **3a**) by a procedure similar to that used to prepare compound **7**. The title compound was obtained as a yellow solid. ^{1}H NMR (300 MHz, DMSO-d_6) δ 8.01 (s, 2H), 7.85 (d, J = 8.2 Hz, 2H), 7.78 (s, 1H), 7.57 (d, J = 8.4 Hz, 2H), 7.36 (s, 1H), 1.32 (s, 9H). ^{13}C NMR (75 MHz, DMSO-d_6) δ 179.11, 169.61, 162.36, 153.99, 131.70 (dd, J = 65.6, 32.8 Hz), 126.50, 125.97, 125.44, 124.22, 121.82, 118.67, 117.72, 114.15, 101.45, 35.14, 31.32. HRMS (ESI) calcd for $C_{24}H_{19}F_6N_4O_2$ 509.1412 $(M + H)^+$, found 519.1410.

4.1.6. N′-(3-Chloro-5-(trifluoromethyl)phenyl)-2-oxo-2-(5-phenylisoxazol-3 yl)acetohydrazonoyl cyanide (13)—Compound **13** was prepared in 47% yield (two steps from **3b**) by a procedure similar to that used to prepare compound **7**. The title compound was obtained as a yellow solid. ^{1}H NMR (300 MHz, DMSO-d_6) δ 7.96 (m, 2H), 7.78 (s, 2H), 7.63 (s, 1H), 7.58 (m, 3H), 7.51 (s, 1H). ^{13}C NMR (75 MHz, DMSO-d_6) δ 179.11, 170.04, 161.55, 145.82, 135.49, 132.65 (q, J = 32.7 Hz), 131.38, 129.80, 126.64, 126.23, 125.27, 121.65, 121.60, 120.93, 114.72, 113.00, 111.19, 102.05. HRMS (ESI) calcd for $C_{19}H_{11}ClF_3N_4O_2$ 419.0523 $(M + H)^+$, found 419.0516.

4.1.7. N-(3-Trifluromethyl-4-chlorophenyl)-2-oxo-2-(5-phenylisoxazol-3-yl)acetohydrazonoyl cyanide (14)—Compound **14** was prepared in 43% yield (two steps from **3b**) by a procedure similar to that used to prepare compound **7**. The title compound was obtained as a yellow solid. ^{1}H NMR (300 MHz, DMSO-d_6) δ 7.96 (d, J = 7.5 Hz, 3H), 7.75 (d, J = 3.0 Hz, 2H), 7.62 – 7.52 (m, 3H), 7.47 (s, 1H). ^{13}C NMR (75 MHz, DMSO-d_6) δ 179.16, 169.93, 161.76, 143.47, 133.29, 131.33, 129.80, 127.93 (q, J = 31.0 Hz), 126.69, 126.22, 124.78, 122.67, 121.16, 116.69, 114.16, 111.57, 101.88. HRMS (ESI) calcd for $C_{19}H_{11}F_3ClN_4O_2$ 419.0523 $(M + H)^+$, found 419.0536.

4.1.8. N-(3,5-Bis(trifluoromethyl)phenyl)-2-oxo-2-(5-phenylisoxazol-3-yl)acetohydrazonoyl cyanide (15)—Compound **15** was prepared in 24% yield (two steps from ethyl 5-phenylisoxazole-3-carboxylate) by a procedure similar to that used to prepare compound **7**. The title compound was obtained as a yellow solid. ^{1}H NMR (300 MHz, DMSO-d_6) δ 8.03 (s, 2H), 7.93 (s, 2H), 7.81 (s, 1H), 7.56 (s, 3H), 7.48 (s, 1H). ^{13}C

NMR (75 MHz, DMSO-d_6) δ 179.09, 169.64, 166.63, 162.17, 131.74 (q, J = 32.8 Hz), 131.24, 129.75, 126.78, 126.13, 125.39, 121.78, 118.42, 117.91, 114.41, 102.06. HRMS (ESI) calcd for $C_{20}H_{11}F_6N_4O_2$ 453.0786 $(M + H)^+$, found 453.0776.

4.1.9. N-(3-Chlorophenyl)-2-(5-(4-fluorophenyl)isoxazol-3-yl)-2-oxoacetohydrazonoyl cyanide (16)—Compound **16** was prepared in 76% yield (two steps from **3c**) by a procedure similar to that used to prepare compound **7**. The title compound was obtained as a yellow solid. ^{1}H NMR (300 MHz, DMSO-d_6) δ 8.10 – 8.02 (m, 2H), 7.57 (s, 1H), 7.52 – 7.39 (m, 5H), 7.26 (d, J = 7.5 Hz, 1H). ^{13}C NMR (75 MHz, DMSO-d_6) δ 179.29, 169.16, 163.89 (d, J = 249.2 Hz), 161.57, 144.28, 134.43, 131.72, 128.97, 128.85, 125.66, 123.42, 117.16, 116.87, 116.23, 113.73, 111.11, 101.90. HRMS (ESI) calcd for $C_{18}H_{11}FClN_4O_2$ 369.0555 $(M + H)^+$, found 369.0549.

4.1.10. N-(3-Chloro-5-(trifluoromethyl)phenyl)-2-(5-(4-fluorophenyl)isoxazol-3-yl)-2-oxoacetohydrazonoyl cyanide (17)—Compound **17** was prepared in 41% yield (two steps from **3c**) by a procedure similar to that used to prepare compound **7**. The title compound was obtained as a yellow solid. ^{1}H NMR (300 MHz, DMSO-d_6) δ 8.04 (dd, J = 8.6, 5.4 Hz, 2H), 7.76 (s, 2H), 7.61 (s, 1H), 7.49 (s, 1H), 7.43 (t, J = 8.8 Hz, 2H). ^{13}C NMR (75 MHz, DMSO-d_6) δ 179.04, 168.95, 163.85 (d, J = 249.1 Hz) 161.89, 135.44, 132.10 (q, J = 32.7 Hz), 128.87, 128.75, 125.32, 123.47, 121.45, 121.20, 117.11, 116.82, 114.45, 113.29, 111.64, 102.00. HRMS (ESI) calcd for $C_{19}H_{10}F_4ClN_4O_2$ 437.0428 $(M + H)^+$, found 437.0420.

4.1.11. N-(4-Chloro-3-(trifluoromethyl)phenyl)-2-(5-(4-fluorophenyl)isoxazol-3-yl)-2-oxoacetohydrazonoyl cyanide (18)—Compound **18** was prepared in 66% yield (two steps from **3c**) by a procedure similar to that used to prepare compound **7**. The title compound was obtained as a yellow solid. ^{1}H NMR (300 MHz, DMSO-d_6) δ 8.08 – 7.96 (m, 3H), 7.82 – 7.71 (m, 2H), 7.49 (s, 1H), 7.43 (t, J = 8.8 Hz, 2H). ^{13}C NMR (75 MHz, DMSO-d_6) δ 179.15, 169.17, 163.87 (d, J = 247.5 Hz), 161.59, 142.56, 133.36, 128.90, 128.79, 126.75, 123.39, 122.34, 117.12, 116.82, 114.30, 111.13, 101.82. HRMS (ESI) calcd for $C_{19}H_{10}F_4ClN_4O_2$ 437.0428 $(M + H)^+$, found 437.0422.

4.1.12. N-(3-Chlorophenyl)-2-(5-(4-chlorophenyl)isoxazol-3-yl)-2-oxoacetohydrazonoyl cyanide (19)—Compound **19** was prepared in 52% yield (two steps from **3d**) by a procedure similar to that used to prepare compound **7**. The title compound was obtained as a yellow solid. ^{1}H NMR (300 MHz, DMSO- d_6) δ 7.99 (d, J = 6.6 Hz, 2H), 7.57 (m, 6H), 7.25 (s, 1H). ^{13}C NMR (75 MHz, DMSO-d_6) δ 179.17, 168.92, 161.62, 144.36, 136.04, 134.43, 131.69, 129.95, 128.10, 125.66, 125.50, 117.18, 116.28, 113.68, 111.15, 102.49. HRMS (ESI) calcd for $C_{18}H_{11}Cl_2N_4O_2$ 385.0259 $(M + H)^+$, found 385.0259.

4.1.13. N-(4-Chloro-3-(trifluoromethyl)phenyl)-2-oxo-2-(5-(4-chlorophenyl)isoxazol-3-yl)acetohydrazonoyl cyanide (20)—Compound **20** was prepared in 81% yield (two steps from **3d**) by a procedure similar to that used to prepare compound **7**. The title compound was obtained as a yellow solid. ^{1}H NMR (300 MHz,

DMSO-d_6) δ 7.98 (d, J = 8.1 Hz, 3H), 7.81–7.70 (m, 2H), 7.64 (d, J = 8.4 Hz, 2H), 7.54 (s, 1H). ^{13}C NMR (75 MHz, DMSO-d_6) δ 179.04, 170.79, 168.96, 161.59, 142.49, 136.02, 133.35, 129.92, 128.17, 128.05, 127.93 (q, J = 31.0 Hz), 125.48, 122.29, 116.57, 114.28, 111.07, 102.44. HRMS (ESI) calcd for $C_{19}H_{10}F_3Cl_2N_4O_2$ 453.0133 $(M + H)^+$, found 453.0130.

4.1.14. N-(3,5-Bis(trifluoromethyl)phenyl)-2-(5-(4-chlorophenyl)isoxazol-3-yl)-2-oxoacetohydrazonoyl cyanide (21)—Compound **21** was prepared in 38% yield (two steps from **3d**) by a procedure similar to that used to prepare compound **7**. The title compound was obtained as a yellow solid. ^{1}H NMR (300 MHz, DMSO) δ 8.06 (s, 2H), 7.97 (d, J = 8.3 Hz, 2H), 7.84 (s, 1H), 7.64 (d, J = 8.2 Hz, 2H), 7.56 (s, 1H). ^{13}C NMR (75 MHz, DMSO) δ 178.96, 168.60, 162.13, 135.91, 131.77 (q, J = 33.1 Hz), 129.88, 127.96, 125.60, 125.37, 121.75, 118.25, 118.01, 102.63. HRMS (ESI) calcd for $C_{20}H_{10}F_6ClN_4O_2$ 487.0396 $(M + H)^+$, found 487.0390.

4.1.15. N-(3-Chlorophenyl)-2-(5-(4-methoxyphenyl)isoxazol-3-yl)-2-oxoacetohydrazonoyl cyanide (22)—Compound **22** was prepared in 56% yield (two steps from **3e**) by a procedure similar to that used to prepare compound **7**. The title compound was obtained as a yellow solid. ^{1}H NMR (300 MHz, DMSO) δ 7.91 (d, J = 8.7 Hz, 2H), 7.57 (s, 1H), 7.52 – 7.42 (m, 2H), 7.33 (s, 1H), 7.25 (d, J = 7.3 Hz, 1H), 7.12 (d, J = 8.8 Hz, 2H), 3.85 (s, 3H). ^{13}C NMR (75 MHz, DMSO) δ 179.46, 170.12, 161.67, 161.46, 134.43, 131.69, 128.06, 125.61, 119.33, 117.17, 116.25, 115.25, 113.75, 100.39, 55.92. HRMS (ESI) calcd for $C_{19}H_{14}ClN_4O_3$ 381.0754 $(M + H)^+$, found 381.0760.

4.1.16. N-(4-Chloro-3-(trifluoromethyl)phenyl)-2-oxo-2-(5-(4-methoxyphenyl)isoxazol-3-yl)acetohydrazonoyl cyanide (23)—Compound **23** was prepared in 33% yield (two steps from **3e**) by a procedure similar to that used to prepare compound **7**. The title compound was obtained as a yellow solid. ^{1}H NMR (300 MHz, DMSO) δ 8.00 (s, 1H), 7.90 (d, J = 8.8 Hz, 2H), 7.81 – 7.70 (m, 2H), 7.34 (s, 1H), 7.12 (d, J = 8.8 Hz, 2H), 3.85 (s, 3H). ^{13}C NMR (75 MHz, DMSO) δ 179.35, 170.15, 161.65, 161.48, 133.35, 128.01, 126.66, 124.76, 122.34, 119.32, 116.70, 116.62, 115.22, 114.32, 100.31, 55.91. HRMS (ESI) calcd for $C_{20}H_{13}F_3ClN_4O_3$ 449.0628 $(M + H)^+$, found 381.0760.

4.1.17. N-(3,5-Bis(trifluoromethyl)phenyl)-2-(5-(4-chlorophenyl)isoxazol-3-yl)-2-oxoacetohydrazonoyl cyanide (24)—Compound **24** was prepared in 14% yield (two steps from **3e**) by a procedure similar to that used to prepare compound **7**. The title compound was obtained as a yellow solid. ^{1}H NMR (300 MHz, DMSO) δ 8.00 (s, 2H), 7.87 (d, J = 8.4 Hz, 2H), 7.78 (s, 1H), 7.28 (s, 1H), 7.10 (d, J = 8.5 Hz, 2H), 3.84 (s, 3H). ^{13}C NMR (75 MHz, DMSO) δ 179.24, 169.56, 162.35, 161.51, 131.69 (q, J = 32.9 Hz), 127.86, 125.44, 121.83, 119.55, 118.63, 117.74, 115.14, 114.16, 100.46, 55.89. HRMS (ESI) calcd for $C_{21}H_{13}F_6N_4O_3$ 483.0892 $(M + H)^+$, found 483.0890.

4.1.18. N-(3-Chlorophenyl)-2-(5-(furan-2-yl)isoxazol-3-yl)-2-oxoacetohydrazonoyl cyanide (25)—To a solution of NaH (197 mg, 4.53 mmol) in anhydrous dioxane (3 mL) was added the solution of ethyl 5-(furan-2-yl)isoxazole-3-

carboxylate **3f** (350 mg, 1.81 mmol) in MeCN (3 mL) dropwise at 0 °C under nitrogen. The solution was stirred at 50 °C for 1 h, and then quenched with sat. NH_4Cl (2 mL) at 0°C. The mixture was poured onto ice/water (10 mL) and extracted with ethyl acetate (20 mL). The organic lay was dried over Na_2SO_4, filtered and concentrated under reduced pressure. The crude residue **4f** (400 mg, quant.) was obtained as a yellow solid and directly used for next step without further purification.

Compound **25** was prepared in 40% yield (two steps from **3f**) by a procedure similar to that used to prepare compound **7**. The title compound was obtained as a yellow solid. ^{1}H NMR (300 MHz, DMSO) δ 8.00 (s, 1H), 7.55 (s, 1H), 7.52 – 7.41 (m, 2H), 7.29 (d, *J* = 3.5 Hz, 1H), 7.25 (d, *J* = 6.7 Hz, 1H), 7.19 (s, 1H), 6.78 (dd, *J* = 3.3, 1.7 Hz, 1H). ^{13}C NMR (75 MHz, DMSO) δ 179.03, 161.57, 161.08, 146.46, 144.03, 141.98, 134.47, 131.72, 125.70, 117.12, 116.10, 113.80, 113.02, 112.68, 110.94, 100.98. HRMS (ESI) calcd for $C_{16}H_{10}ClN_4O_3$ 341.0441 $(M + H)^+$, found 341.0444.

4.1.19. N-(3-Chloro-5-(trifluoromethyl)phenyl)-2-(5-(furan-2-yl)isoxazol-3-yl)-2-oxoacetohydrazonoyl cyanide (26)—Compound **26** was prepared in 38% yield (two steps from **3f**) by a procedure similar to that used to prepare compound **25**. The title compound was obtained as a yellow solid. ^{1}H NMR (300 MHz, DMSO) δ 7.99 (d, *J* = 1.7 Hz, 1H), 7.76 (s, 2H), 7.62 (s, 1H), 7.27 (d, *J* = 3.5 Hz, 1H), 7.20 (s, 1H), 6.77 (dd, *J* = 3.5, 1.8 Hz, 1H). ^{13}C NMR (75 MHz, DMSO) δ 178.78, 161.50, 161.21, 146.42, 141.99, 135.52, 132.19 (d, *J* = 32.9 Hz), 125.26, 121.65, 120.94, 114.68, 112.98, 112.56, 101.10. HRMS (ESI) calcd for $C_{17}H_9F_3ClN_4O_3$ 409.0315 $(M + H)^+$, found 409.0310.

4.1.20. N-(4-Chloro-3-(trifluoromethyl)phenyl)-2-(5-(furan-2-yl)isoxazol-3-yl)-2-oxoacetohydrazonoyl cyanide (27)—Compound **27** was prepared in 36% yield (two steps from **3f**) by a procedure similar to that used to prepare compound **25**. The title compound was obtained as a yellow solid. 1H NMR (300 MHz, DMSO) δ 8.00 (d, *J* = 1.7 Hz, 1H), 7.96 (d, *J* = 2.1 Hz, 1H), 7.79 (d, *J* = 8.7 Hz, 1H), 7.76 – 7.69 (m, 1H), 7.27 (d, *J* = 3.6 Hz, 1H), 7.19 (s, 1H), 6.78 (dd, *J* = 3.5, 1.8 Hz, 1H). ^{13}C NMR (75 MHz, DMSO) δ 178.89, 161.52, 161.24, 146.41, 142.86, 142.01, 133.37, 128.00 (q, *J* = 31.1 Hz), 126.73, 124.75, 122.44, 121.14, 116.65, 116.58, 114.30, 112.99, 112.58, 111.19, 100.96. HRMS (ESI) calcd for $C_{17}H_9F_3ClN_4O_3$ 409.0315 $(M + H)^+$, found 409.0312.

4.1.21. 2-(Benzo[d]isoxazol-3-yl)-N-(3-chlorophenyl)-2-oxoacetohydrazonoyl cyanide (30)—To a solution of CH_3CN (0.46 mL, 8.80 mmol) in anhydrous THF (8 mL) was added 1.6 M methyl lithium in diethyl ether (2.75 mL, 4.40 mmol) at −78 °C under nitrogen. The mixture was stirred at −78 °C for 0.5 h, and ethyl benzo[*d*]isoxazole-3-carboxylate **28** (420 mg g, 2.20 mmol) in THF (10 mL) was then added dropwise. The solution was stirred at −78 °C for 1 h and then quenched with acetic acid (0.26 mL, 4.40 mmol). The mixture was warmed to 0 °C and poured onto ice/water (10 mL) and extracted with ethyl acetate (20 mL). The organic lay was dried over Na_2SO_4, filtered and concentrated under reduced pressure. The crude residue **29** (400 mg, 98%) was obtained as a yellow solid and directly used for next step without further purification. ^{1}H NMR (300 MHz, $CDCl_3$) δ 8.24 (d, *J* = 8.0 Hz, 1H), 7.77 – 7.66 (m, 2H), 7.57 – 7.49 (m, 1H), 4.40 (s,

2H). ^{13}C NMR (75 MHz, $CDCl_3$) δ 182.38, 164.73, 131.23, 126.16, 123.23, 118.36, 112.60, 110.18, 30.34.

Compound **30** was prepared in 53% yield (two steps from **28**) by a procedure similar to that used to prepare compound **7**. The title compound was obtained as a yellow solid. ^{1}H NMR (300 MHz, DMSO-d_6) δ 8.05 (d, J = 8.1 Hz, 1H), 7.94 (d, J = 8.6 Hz, 1H), 7.77 (t, J = 7.7 Hz, 1H), 7.51 (t, J = 7.5 Hz, 1H), 7.44 – 7.33 (m, 3H), 7.26 – 7.19 (m, 1H). ^{13}C NMR (75 MHz, DMSO-d_6) δ 179.64, 162.99, 155.16, 144.19, 134.42, 131.65, 131.50, 125.70, 125.65, 123.74, 120.52, 116.96, 116.15, 113.98, 111.13, 110.42. HRMS (ESI) calcd for $C_{16}H_{10}ClN_4O_2$ 325.0492 $(M + H)^+$, found 325.0483.

4.1.22. 2-(Benzo[d]isoxazol-3-yl)-N-(3-chloro-5-(trifluoromethyl)phenyl)-2-oxoacetohydrazonoyl cyanide (31)—Compound **31** was prepared in 33% yield (two steps from **28**) by a procedure similar to that used to prepare compound **30**. The title compound was obtained as a yellow solid. ^{1}H NMR (300 MHz, DMSO-d_6) δ 8.04 (d, J = 8.0 Hz, 1H), 7.94 (d, J = 8.4 Hz, 1H), 7.76 (t, J = 7.7 Hz, 1H), 7.60 (s, 3H), 7.49 (t, J = 7.6 Hz, 1H). ^{13}C NMR (75 MHz, DMSO-d_6) δ 179.40, 163.00, 155.37, 145.94, 135.46, 132.12 (q, J = 32.8 Hz), 131.44, 125.63, 123.76, 121.59, 120.85, 120.56, 114.90, 112.83, 111.28, 110.39. HRMS (ESI) calcd for $C_{17}H_9F_3ClN_4O_2$ 393.0366 $(M + H)^+$, found 393.0376.

4.1.23. 2-(Benzo[d]isoxazol-3-yl)-N-(3-chloro-4-(trifluoromethyl)phenyl)-2-oxoacetohydrazonoyl cyanide (32)—Compound **32** was prepared in 22% yield (two steps from **28**) by a procedure similar to that used to prepare compound **30**. The title compound was obtained as a yellow solid. ^{1}H NMR (300 MHz, DMSO-d_6) δ 8.02 (d, J = 8.1 Hz, 1H), 7.93 (d, J = 8.7 Hz, 1H), 7.84 (d, J = 8.4 Hz, 1H), 7.76 (t, J = 7.8 Hz, 1H), 7.56 – 7.42 (m, 3H). ^{13}C NMR (75 MHz, DMSO-d_6) δ 179.41, 162.96, 132.27, 132.25, 131.44, 129.75, 129.68, 125.61, 123.72, 120.61, 119.55, 116.47, 115.39, 110.39. HRMS (ESI) calcd for $C_{17}H_9F_3ClN_4O_2$ 393.0366 $(M + H)^+$, found 393.0378.

4.1.24. 2-(Benzo[d]isoxazol-3-yl)-N-(4-chloro-3-(trifluoromethyl)phenyl)-2-oxoacetohydrazonoyl cyanide (33)—Compound **33** was prepared in 55% yield (two steps from **28**) by a procedure similar to that used to prepare compound **30**. The title compound was obtained as a yellow solid. ^{1}H NMR (300 MHz, DMSO-d_6) δ 8.02 (d, J = 8.0 Hz, 1H), 7.92 (d, J = 8.5 Hz, 1H), 7.81 – 7.69 (m, 3H), 7.63 (dd, J = 9.0, 2.2 Hz, 1H), 7.48 (t, J = 7.5 Hz, 1H). ^{13}C NMR (75 MHz, DMSO-d_6) δ 179.43, 163.01, 155.19, 142.68, 133.29, 131.43, 127.96 (q, J = 31.2 Hz), 126.77, 125.61, 124.68, 123.66, 122.34, 121.06, 120.53, 116.45, 116.37, 114.51, 111.19, 110.36. HRMS (ESI) calcd for $C_{17}H_9F_3ClN_4O_2$ 393.0366 $(M + H)^+$, found 393.0374.

4.1.25. 2-(Benzo[d]isoxazol-3-yl)-N-(3-chloro-5-fluorophenyl)-2-oxoacetohydrazonoyl cyanide (34)—Compound **34** was prepared in 57% yield (two steps from **28**) by a procedure similar to that used to prepare compound **30**. The title compound was obtained as a yellow solid. ^{1}H NMR (300 MHz, DMSO-d_6) δ 8.04 (d, J = 7.9 Hz, 1H), 7.92 (d, J = 8.5 Hz, 1H), 7.76 (t, J = 7.7 Hz, 1H), 7.50 (t, J = 7.5 Hz, 1H), 7.24 – 7.16 (m, 2H), 7.11 (d, J = 10.3 Hz, 1H). ^{13}C NMR (75 MHz, DMSO-d_6) δ 179.43, 162.99, 162.98 (d, J = 245.0 Hz), 155.13, 146.02, 135.30 (d, J = 5.9 Hz), 131.47, 125.66, 123.77,

120.54, 114.60, 113.59, 112.99, 112.65, 111.16, 110.43, 103.49 (d, J = 26.6 Hz). HRMS (ESI) calcd for $C_{16}H_9FClN_4O_2$ 343.0398 $(M + H)^+$, found 343.0388.

4.1.26. 2-(Benzo[d]isoxazol-3-yl)-N-(3-chloro-4-fluorophenyl)-2-oxoacetohydrazonoyl cyanide (35)—Compound **35** was prepared in 44% yield (two steps from **28**) by a procedure similar to that used to prepare compound **30**. The title compound was obtained as a yellow solid. ^{1}H NMR (300 MHz, DMSO-d_6) δ 8.04 (d, J = 8.0 Hz, 1H), 7.92 (d, J = 8.5 Hz, 1H), 7.80 – 7.72 (m, 1H), 7.54–7.36 (m, 4H). ^{13}C NMR (75 MHz, DMSO-d_6) δ 179.48, 162.99, 155.29 (d, J = 240. 0 Hz), 155.07, 140.15, 131.46, 125.64, 123.70, 121.00, 120.74, 120.53, 118.95, 118.38, 118.08, 117.90, 117.80, 113.78, 111.15, 110.40. HRMS (ESI) calcd for $C_{16}H_9FClN_4O_2$ 343.0398 $(M + H)^+$, found 343.0387.

4.1.27. 2-(Benzo[d]isoxazol-3-yl)-N-(3,5-bis(trifluoromethyl)phenyl)-2-oxoacetohydrazonoyl cyanide (36)—Compound **36** was prepared in 31% yield (two steps from **28**) by a procedure similar to that used to prepare compound **30**. The title compound was obtained as a yellow solid. ^{1}H NMR (300 MHz, DMSO-d_6) δ 8.02 (d, J = 7.9 Hz, 1H), 7.93 (d, J = 8.5 Hz, 1H), 7.88 (s, 2H), 7.81 (s, 1H), 7.75 (t, J = 7.8 Hz, 1H), 7.47 (t, J = 7.6 Hz, 1H). ^{13}C NMR (75 MHz, DMSO-d_6) δ 179.35, 162.99, 155.56, 146.13, 132.83 (q, J = 32.9 Hz), 131.37, 125.55, 125.24, 123.70, 121.62, 120.59, 117.75, 115.06, 111.39, 110.34. HRMS (ESI) calcd for $C_{18}H_9F_6N_4O_2$ 427.0630 $(M + H)^+$, found 427.0617.

4.1.28. 2-(Benzo[d]isoxazol-3-yl)-N-(3,4,5-trifluorophenyl)-2-oxoacetohydrazonoyl cyanide (37)—Compound **37** was prepared in 25% yield (two steps from **28**) by a procedure similar to that used to prepare compound **30**. The title compound was obtained as a brown solid. ^{1}H NMR (300 MHz, DMSO-d_6) δ 8.02 (d, J = 7.7 Hz, 1H), 7.91 (d, J = 8.6 Hz, 1H), 7.76 (t, J = 7.7 Hz, 1H), 7.50 (t, J = 7.5 Hz, 1H), 7.17 (dd, J = 9.1, 6.8 Hz, 2H). ^{13}C NMR (75 MHz, DMSO-d_6) δ 179.20, 170.81, 162.92, 155.28, 151.14 (ddd, J = 246.5, 10.5, 5.0 Hz), 140.66, 138.18, 135.11, 131.39, 125.58, 123.71, 120.64, 114.17, 111.60, 110.41, 102.22 (d, J = 24.6 Hz). HRMS (ESI) calcd for $C_{16}H_8F_3N_4O_2$ 345.0599 $(M + H)^+$, found 345.0590.

4.2. In vitro guanine nucleotide exchange factor (GEF) activity assay of EPAC proteins

In vitro EPAC GEF activity was acquired as previously described [25]. Briefly, the assay was performed using 500 nM Rap1b-BODIPY-GDP and 200 nM EPAC proteins in buffer containing 50 mM Tris-HCl pH 7.5, 50 mM NaCl, 5 mM $MgCl_2$, 1 mM DTT, 50 mM GDP and the indicated concentrations of test compounds at room temperature using half-area 96-well plates (Corning Costar 3915). The exchange reaction was monitored using a Spectramax M2 Plate Reader (Molecular Devices) with the excitation/emission wavelengths set at 485/515 nm. The reaction rate constant (k_{obs}) was determined by globally fitting the experimental data to a single exponential equation. Quantification was processed by nominalizing the observed k_{obs} in the presence of inhibitor with the rate constant in the presence of 20 μM cAMP (no inhibitor) (k_{cAMP}) and the rate constant without cAMP or inhibitor (k_0) using equation: $Relative\ GEF\ activity = (k_{obs} - k_0)/(k_{cAMP} - k_0) \times 100$.

4.3. Molecular docking studies

The docking study was performed with Schrödinger Small-Molecule Drug Discovery Suite [29]. The crystal structure of EPAC2 (PDB code: 3CF6) was downloaded from RCSB PDB Bank and prepared with Protein Prepared Wizard [30]. During this step, hydrogens were added, crystal waters were removed, and partial charges were assigned using the OPLS-2005 force field. The 3D structures of **1** (**ESI-09**), **10** (**NY0617**) and **33** (**NY0562**) were created with Schrödinger Maestro [31] and the initial lowest energy conformations were calculated with LigPrep [32]. For all dockings, the grid center was chosen on the centroid of included ligand of PDB structure CBD-B site and a 24 × 24 × 24 Å grid box size was used. All dockings were employed with Glide [33] using the XP protocol. Docking poses were incorporated into Schrödinger Maestro for a visualization of ligand-receptor interactions and overlay analysis.

Supplementary Material

Refer to Web version on PubMed Central for supplementary material.

Acknowledgments

This work was supported by grants R01 GM106218, R01 AI111464, and R01 GM066170 from the National Institutes of Health. We want to thank Drs. Lawrence C. Sowers and Cheryl F. Lichti at the Department of Pharmacology as well as Dr. Tianzhi Wang at the NMR core facility of UTMB for the NMR spectroscopy assistance.

Abbreviations

EPAC	exchange proteins directly activated by cAMP
SAR	structure-activity relationship
cAMP	cyclic adenosine monophosphate
8-NBD-cAMP	8-(2-[7-nitro-4-benzofurazanyl]aminoethylthio)adenosine-3′,5′-cyclic monophosphate
GDP	guanosine diphosphate
PKA	protein kinase A
GEF	guanine nucleotide exchange factor
GTP	guanosine triphosphate
Rap	Ras-related protein
HTS	high-throughput screening
TLC	thin layer chromatography
UV	ultraviolet

TMS	tetramethylsilane
HRMS	high-resolution mass spectrometry
HPLC	high-performance liquid chromatography
DCM	dichloromethane
EtOAc	ethyl acetate
DMSO	dimethyl sulfoxide
EDTA	ethylenediaminetetraacetic acid
DDT	dichlorodiphenyltrichloroethane
ADP	adenosine diphosphate
CBD	cAMP binding domain

References

1. de Rooij J, Zwartkruis FJ, Verheijen MH, Cool RH, Nijman SM, Wittinghofer A, Bos JL. Epac is a Rap1 guanine-nucleotide-exchange factor directly activated by cyclic AMP. Nature. 1998; 396:474–477. [PubMed: 9853756]
2. Kawasaki H, Springett GM, Mochizuki N, Toki S, Nakaya M, Matsuda M, Housman DE, Graybiel AM. A family of cAMP-binding proteins that directly activate Rap1. Science. 1998; 282:2275–2279. [PubMed: 9856955]
3. Cohen P. Protein kinases--the major drug targets of the twenty-first century? Nat Rev Drug Discov. 2002; 1:309–315. [PubMed: 12120282]
4. Zambon AC, Zhang L, Minovitsky S, Kanter JR, Prabhakar S, Salomonis N, Vranizan K, Dubchak I, Conklin BR, Insel PA. Gene expression patterns define key transcriptional events in cell-cycle regulation by cAMP and protein kinase A. Proc Natl Acad Sci U S A. 2005; 102:8561–8566. [PubMed: 15939874]
5. Biel M. Cyclic nucleotide-regulated cation channels. J Biol Chem. 2009; 284:9017–9021. [PubMed: 19054768]
6. Biel M, Michalakis S. Cyclic nucleotide-gated channels. Handb Exp Pharmacol. 2009:111–136.
7. Chen H, Wild C, Zhou X, Ye N, Cheng X, Zhou J. Recent advances in the discovery of small molecules targeting exchange proteins directly activated by cAMP (EPAC). J Med Chem. 2014; 57:3651–3665. [PubMed: 24256330]
8. Wang P, Liu Z, Chen H, Ye N, Cheng X, Zhou J. Exchange proteins directly activated by cAMP (EPACs): Emerging therapeutic targets. Bioorg Med Chem Lett. 2017; 27:1633–1639. [PubMed: 28283242]
9. Vliem MJ, Ponsioen B, Schwede F, Pannekoek WJ, Riedl J, Kooistra MR, Jalink K, Genieser HG, Bos JL, Rehmann H. 8-pCPT-2′-O-Me-cAMP-AM: an improved Epac-selective cAMP analogue. ChemBioChem. 2008; 9:2052–2054. [PubMed: 18633951]
10. Tsalkova T, Mei FC, Cheng X. A fluorescence-based high-throughput assay for the discovery of exchange protein directly activated by cyclic AMP (EPAC) antagonists. PLoS One. 2012; 7:e30441. [PubMed: 22276201]
11. Tsalkova T, Mei FC, Li S, Chepurny OG, Leech CA, Liu T, Holz GG, Woods VL Jr, Cheng X. Isoform-specific antagonists of exchange proteins directly activated by cAMP. Proc Natl Acad Sci U S A. 2012; 109:18613–18618. [PubMed: 23091014]
12. Almahariq M, Tsalkova T, Mei FC, Chen H, Zhou J, Sastry SK, Schwede F, Cheng X. A novel EPAC-specific inhibitor suppresses pancreatic cancer cell migration and invasion. Mol Pharmacol. 2013; 83:122–128. [PubMed: 23066090]

13. Gong B, Shelite T, Mei FC, Ha T, Hu Y, Xu G, Chang Q, Wakamiya M, Ksiazek TG, Boor PJ, Bouyer DH, Popov VL, Chen J, Walker DH, Cheng X. Exchange protein directly activated by cAMP plays a critical role in bacterial invasion during fatal rickettsioses. Proc Natl Acad Sci U S A. 2013; 110:19615–19620. [PubMed: 24218580]
14. Almahariq M, Mei FC, Wang H, Cao AT, Yao S, Soong L, Sun J, Cong Y, Chen J, Cheng X. Exchange protein directly activated by cAMP modulates regulatory T-cell-mediated immunosuppression. Biochem J. 2015; 465:295–303. [PubMed: 25339598]
15. Grandoch M, Roscioni SS, Schmidt M. The role of Epac proteins, novel cAMP mediators, in the regulation of immune, lung and neuronal function. Br J Pharmacol. 2010; 159:265–284. [PubMed: 19912228]
16. Breckler M, Berthouze M, Laurent AC, Crozatier B, Morel E, Lezoualc'h F. Rap-linked cAMP signaling Epac proteins: compartmentation, functioning and disease implications. Cell Signalling. 2011; 23:1257–1266. [PubMed: 21402149]
17. Gloerich M, Bos JL. Epac: defining a new mechanism for cAMP action. Annu Rev Pharmacol Toxicol. 2010; 50:355–375. [PubMed: 20055708]
18. Almahariq M, Chao C, Mei FC, Hellmich MR, Partikeev I, Motamedi M, Cheng X. Pharmacological inhibition and genetic knockdown of EPAC1 reduce pancreatic cancer metastasis in vivo. Mol Pharmacol. 2015; 87:142–149. [PubMed: 25385424]
19. Schmidt M, Dekker FJ, Maarsingh H. Exchange protein directly activated by cAMP (epac): a multidomain cAMP mediator in the regulation of diverse biological functions. Pharmacol Rev. 2013; 65:670–709. [PubMed: 23447132]
20. Chen H, Ding C, Wild C, Liu H, Wang T, White MA, Cheng X, Zhou J. Efficient synthesis of ESI-09, a novel non-cyclic nucleotide EPAC antagonist. Tetrahedron Lett. 2013; 54:1546–1549. [PubMed: 23459418]
21. Chen H, Tsalkova T, Chepurny OG, Mei FC, Holz GG, Cheng X, Zhou J. Identification and characterization of small molecules as potent and specific EPAC2 antagonists. J Med Chem. 2013; 56:952–962. [PubMed: 23286832]
22. Chen H, Tsalkova T, Mei FC, Hu Y, Cheng X, Zhou J. 5-Cyano-6-oxo-1, 6-dihydro-pyrimidines as potent antagonists targeting exchange proteins directly activated by cAMP. Bioorg Med Chem Lett. 2012; 22:4038–4043. [PubMed: 22607683]
23. Wild CT, Zhu Y, Na Y, Mei F, Ynalvez MA, Chen H, Cheng X, Zhou J. Functionalized N, N-diphenylamines as potent and selective EPAC2 inhibitors. ACS Med Chem Lett. 2016; 7:460–464. [PubMed: 27190593]
24. Ye N, Zhu Y, Chen H, Liu Z, Mei FC, Wild C, Chen H, Cheng X, Zhou J. Structure-activity relationship studies of substituted 2-(isoxazol-3-yl)-2-oxo-N′-phenyl-acetohydrazonoyl cyanide analogues: identification of potent exchange proteins directly activated by cAMP (EPAC) antagonists. J Med Chem. 2015; 58:6033–6047. [PubMed: 26151319]
25. Zhu Y, Chen H, Boulton S, Mei F, Ye N, Melacini G, Zhou J, Cheng X. Biochemical and pharmacological characterizations of ESI-09 based EPAC inhibitors: defining the ESI-09 "therapeutic window". Sci Rep. 2015; 5:9344. [PubMed: 25791905]
26. Ye N, Chen CH, Chen T, Song Z, He JX, Huan XJ, Song SS, Liu Q, Chen Y, Ding J, Xu Y, Miao ZH, Zhang A. Design, synthesis, and biological evaluation of a series of benzo[de][1, 7]naphthyridin-7(8H)-ones bearing a functionalized longer chain appendage as novel PARP1 inhibitors. J Med Chem. 2013; 56:2885–2903. [PubMed: 23473053]
27. Rehmann H, Das J, Knipscheer P, Wittinghofer A, Bos JL. Structure of the cyclic-AMP-responsive exchange factor Epac2 in its auto-inhibited state. Nature. 2006; 439:625–628. [PubMed: 16452984]
28. Rehmann H, Arias-Palomo E, Hadders MA, Schwede F, Llorca O, Bos JL. Structure of Epac2 in complex with a cyclic AMP analogue and RAP1B. Nature. 2008; 455:124–127. [PubMed: 18660803]
29. Small-Molecule Drug Discovery Suite 2016–4. Schrödinger, LLC; New York, NY: 2016.
30. Schrödinger Release 2016–4: Schrödinger Suite 2016–4 Protein Preparation Wizard. Schrödinger, LLC; New York, NY: 2016.
31. Schrödinger Release 2016–4: Maestro. Schrödinger, LLC; New York, NY: 2016.

32. Schrödinger Release 2016–4: LigPrep. Schrödinger, LLC; New York, NY: 2016.
33. Schrödinger Release 2016–4: Glide. Schrödinger, LLC; New York, NY: 2016.

Appendix A. Supplementary data

Supplementary data related to this article can be found at http://dx.doi.org/10.1016/j.ejmech.xxxx.xx.xxx.

Highlights

- Further structural modifications and SAR studies based on **ESI-09** are presented.
- Two series of novel diversified analogues have been designed and synthesized.
- **14, 32** and **33** identified as potent EPAC antagonists with low micromolar activities.
- Molcular dockings on ligand-EPAC2 protein binding interactions are explored.
- Benzo[*d*]isoxazol analogues offer new lead scaffolds for further optimization.

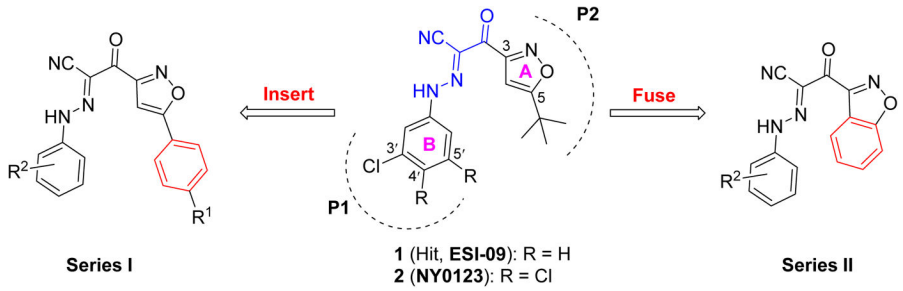

Fig. 1.
Drug design strategy for the current work.

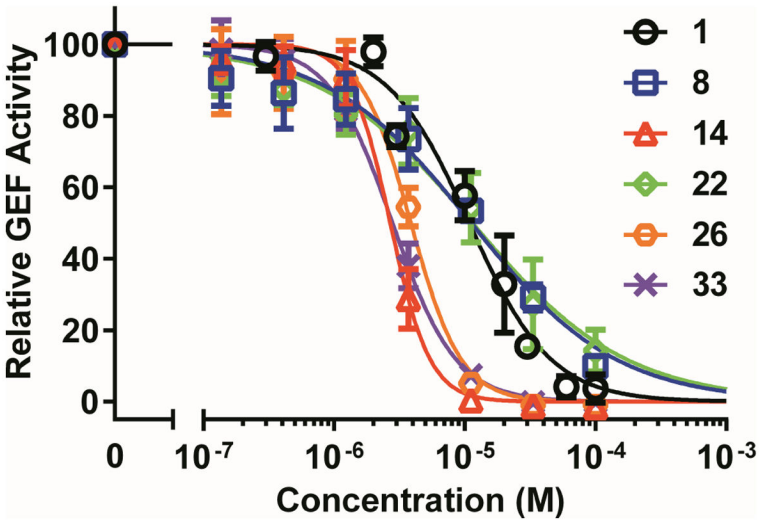

Fig. 2.

Relative inhibitory activity for EPAC1-mediated Rap1b-bGDP exchange. Dose-dependent inhibition of EPAC1 GEF activity by compound **1** (black), **8** (blue), **14** (red), **22** (green), **26** (brown) and **33** (purple), in the presence of 20 μM cAMP. Relative GEF activity were presented as normalized reaction rate constant (means ± SD, n = 3) described in the method.

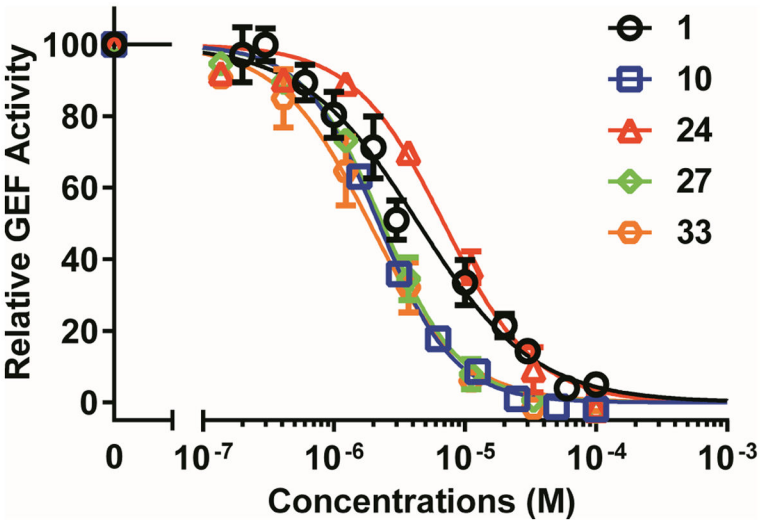

Fig. 3.

Relative inhibitory activity for EPAC2-mediated Rap1b-bGDP exchange. Dose-dependent inhibition of EPAC2 GEF activity by compound **1** (black), **10** (blue), **24** (red), **27** (green), **33** (brown), in the presence of 20 μM cAMP. Relative GEF activity were presented as normalized reaction rate constant (means ± SD, n =3) described in the method.

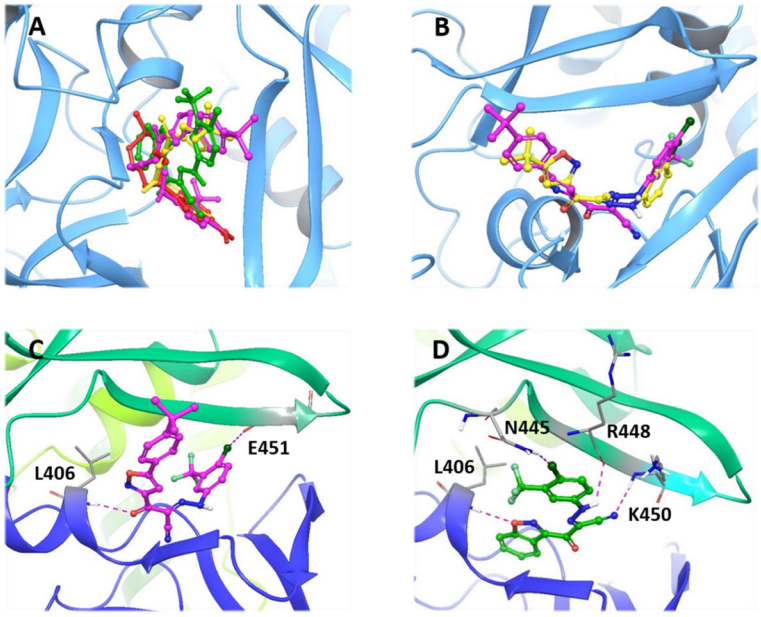

Fig. 4.

(A) Overlay analysis of molecular docking poses of **1**, **10** and **33** binding at the cAMP binding domain B (CBD-B) of EPAC2 protein (PDB Code 3CF6). cAMP is shown in red, **1** in yellow, **10** in magenta, and **33** in green. (B) Overlay of molecular docking poses of **1** (yellow) and **10** (magenta) binding at the CBD-B of EPAC2. (C) Predicted binding mode of **10** docked into the CBD-B of EPAC2. **10** is shown in magenta ball and stick representation. Key residues are displayed in sticks. Hydrogen bonds and halogen bond are shown in dotted purple lines. (D) Predicted binding mode of **33** docked into the CBD-B of EPAC2. **33** is shown in green ball and stick representation. Key residues are displayed in sticks. Hydrogen bonds and halogen bond are shown in dotted purple lines.

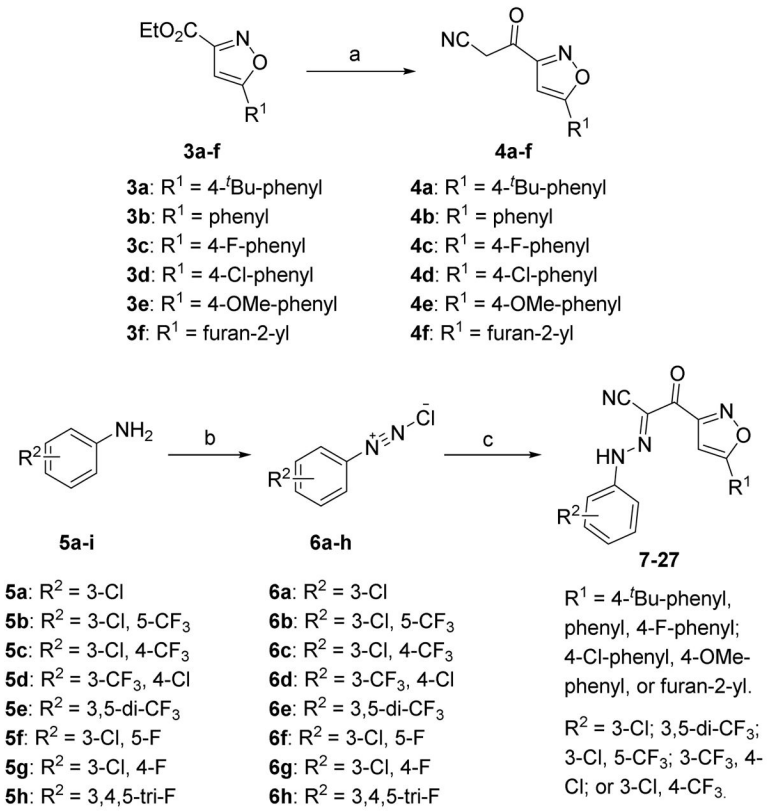

Scheme 1.

Synthesis of the 2-oxo-*N*-phenyl-2-(5-phenylisoxazol-3-yl)acetohydrazonoyl cyanide analogues **7–27**. Reagents and conditions: (a) CH_3CN, MeLi, THF, -78 °C; or CH_3CN, NaH, THF, 50 °C; (b) 2 N HCl, $NaNO_2$, H_2O, 0 °C; (c) **4a–f**, NaOAc, EtOH, 14–81% for three steps.

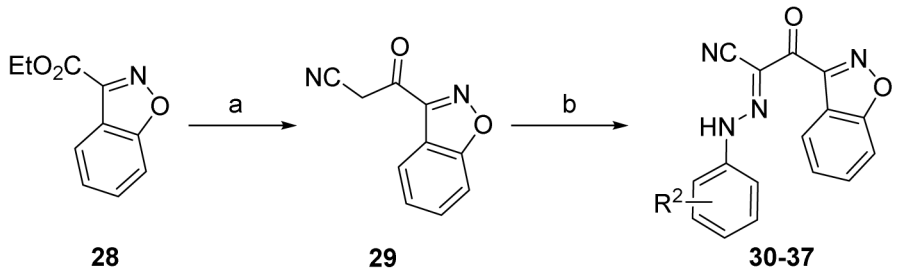

For compounds **30** - **37**: R^2 = 3-Cl; 3,5-di-CF_3; 3-Cl, 5-CF_3; 3-F, 5-Cl; 3-Cl, 4-F; 3-CF_3, 4-Cl; 3-Cl, 4-CF_3; 3,4,5-tri-F.

Scheme 2.

Synthesis of 2-(benzo[*d*]isoxazol-3-yl)-2-oxo-*N*-phenylacetohydrazonoyl Cyanide Analogues **30–37**. Reagents and conditions: (a) CH_3CN, MeLi, THF, −78 °C; (b) **6a–h**, NaOAc, EtOH, 22–57% for two steps.

Table 1

Apparent IC_{50} values of substituted 2-(isoxazol-3-yl)-2-oxo-*N*′-phenyl-acetohydrazonoyl cyanide scaffolds for inhibiting EPAC1 GEF activity.

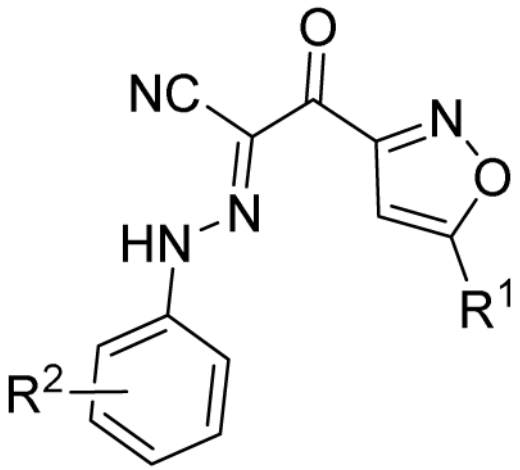

Compound	R^1	R^2	Rap1b-bGDP EPAC1 IC_{50} (μM)[a]
1			10.8 ± 1.6
7	4-^{t}Bu-phenyl	3-Cl	8.6 ± 2.8
8	4-^{t}Bu-phenyl	3-Cl, 5-CF_3	10.2 ± 2.7
9	4-^{t}Bu-phenyl	3-Cl, 4-CF_3	9.0 ± 3.9
10	4-^{t}Bu-phenyl	3-CF_3, 4-Cl	7.3 ± 2.3
11	4-^{t}Bu-phenyl	3, 5-di-CF_3	11.9 ± 6.0
12	phenyl	3-Cl	>150
13	phenyl	3-Cl, 5-CF_3	9.5 ± 1.2
14	phenyl	3-CF_3, 4-Cl	2.4 ± 0.2
15	phenyl	3, 5-di-CF_3	7.2 ± 0.7
16	4-F-phenyl	3-Cl	38.6 ± 7.7
17	4-F-phenyl	3-Cl, 5-CF_3	12.7 ± 1.1
18	4-F-phenyl	3-CF_3, 4-Cl	10.2 ± 0.8
19	4-Cl-phenyl	3-Cl	77.6 ± 35.8
20	4-Cl-phenyl	3-CF_3, 4-Cl	7.8 ± 2.1
21	4-Cl-phenyl	3, 5-di-CF_3	11.4 ± 2.7
22	4-OMe-phenyl	3-Cl	11.4 ± 2.8
23	4-OMe-phenyl	3-CF_3, 4-Cl	5.6 ± 1.1
24	4-OMe-phenyl	3, 5-di-CF_3	5.6 ± 1.0
25	furan-2-yl	3-Cl	9.9 ± 3.3
26	furan-2-yl	3-Cl, 5-CF_3	3.6 ± 0.2
27	furan-2-yl	3-CF_3, 4-Cl	4.2 ± 0.9

[a]The values are the mean ± SD of at least three independent experiments.

Table 2

Apparent IC_{50} values of substituted 2-(isoxazol-3-yl)-2-oxo-*N*′-phenyl-acetohydrazonoyl cyanide scaffolds for inhibiting EPAC1 GEF activity.

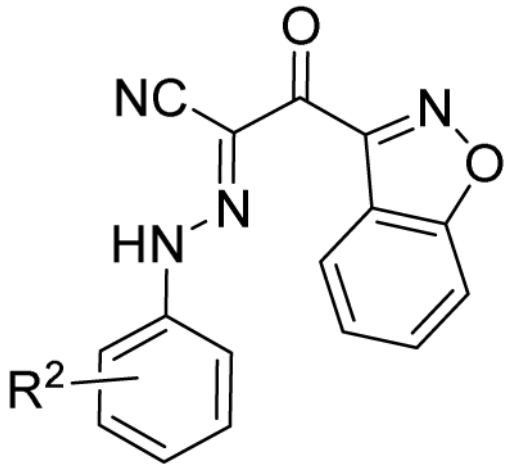

Compound	R^2	Rap1b-bGDP EPAC1 IC_{50} (μM)[a]
30	3-Cl	13.2 ± 3.6
31	3-Cl, 5-CF_3	4.6 ± 0.8
32	3-Cl, 4-CF_3	3.0 ± 0.3
33	3-CF_3, 4-Cl	2.7 ±0.3
34	3-Cl, 5-F	18.9 ± 4.9
35	3-Cl, 4-F	8.5 ± 3.5
36	3,5-di-CF_3	6.7 ± 0.7
37	3,4,5-tri-F	13.1 ± 2.5

[a]The values are the mean ± SD of at least three independent experiments.

Table 3

Apparent IC_{50} values of substituted 2-(isoxazol-3-yl)-2-oxo-*N*′-phenyl-acetohydrazonoyl cyanide scaffolds for inhibiting EPAC2 GEF activity.

Compound	Rap1b-bGDP EPAC2 IC_{50} (μM)[a]
1	4.4 ± 0.5
10	2.2 ± 0.3
14	2.3 ± 0.5
15	3.3 ± 0.8
23	4.5 ± 1.0
24	7.0 ± 0.9
26	2.2 ± 0.3
27	2.3 ± 0.2
31	2.2 ± 0.2
32	2.2 ± 0.4
33	1.9 ± 0.3

[a]The values are the mean ± SD of at least three independent experiments.